Chapter 3

Hydrogen bond symmetrization in δ-AlOOH

3.1 Introduction

Water and water bearing minerals play an important role in geodynamics and various geophysical phenomena. If water is carried and released into the deep mantle, various properties of mantle constituents such as elasticity, melting temperature, viscosity, etc would be considerably affected. Even though most of the hydrous minerals lose water at high-pressure-temperature condition, the presence of H-bearing mineral phases at lower mantle conditions is now confirmed with solid evidences [80, 81]. Therefore, the high-pressure behaviour of hydrous minerals enables understanding the geochemical evolution of the Earth. Hydrated magnesium silicates, i.e phases in (MgO/Al_2O_3)-SiO_2-H_2O systems are thought to be important water resources in the lower mantle. The existence of aluminous hydrous silicate, phase Egg ($AlSiO_3(OH)$) in Earth's interior has been confirmed from its presence in inclusions of natural diamonds [28]. It undergoes decomposition to form δ-AlOOH and stishovite under the pressure-temperature condition of mantle transition zone [43] which makes δ-AlOOH an important candidate for carrying water to the lower mantle [82].

δ-AlOOH was first synthesised by Suzuki et al. [83] at 21 GPa and 1000 ℃. At ambient conditions, δ-AlOOH exhibits orthorhombic symmetric structure with $P21nm$ space group

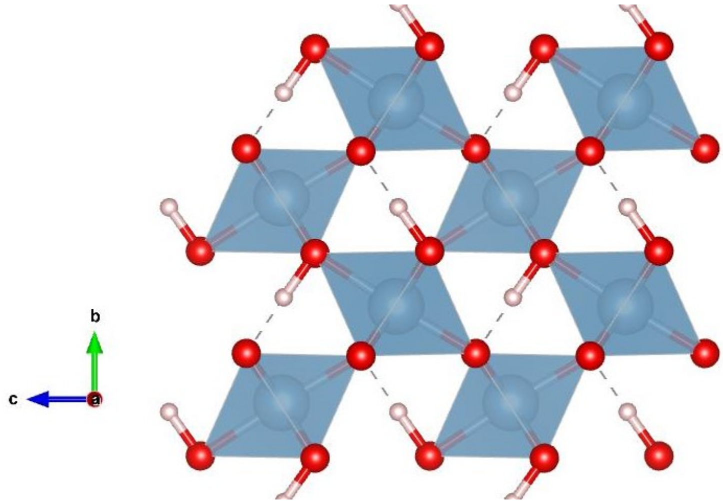

Figure 3.1: Ball and stick model of structure of δ-AlOOH at 0 GPa. Red and grey spheres represent oxygen and hydrogen atom respectively. AlO_6 polyhedra is shown in blue

[83–85]. The crystal structure consists of AlO_6 octahedra joined via corners as shown in Fig. 3.1. This configuration gives rise to the formation of a hydrogen bond between oxygens belonging to non-adjacent octahedra and lies along the *a*-*b* plane. In general, hydrogen bond has asymmetric O-H--O configuration at ambient condition comprising of a short covalent O-H bond and a long O--H hydrogen bond. Under compression, the double well structure of the potential surface between two oxygen atoms transforms to the single minimum surface thereby driving the hydrogen atom to the centre of the O--O vector, and this process is called symmetrization of hydrogen bond [37]. In the case of δ-AlOOH, even though it has been subjected to many experimental [28, 44, 81, 83, 85] and theoretical [41–43, 86] investigations, the pressure at which hydrogen bond symmetrization occurs have been debated for long. At ambient condition, the hydrogen bonds in δ-AlOOH are asymmetric [85, 87]. The first study on hydrogen bond symmetrization in δ-AlOOH was carried out theoretically by Tsuchiya et al. [41] using first principles calculations where the phase of δ-AlOOH with asymmetric hydrogen bond at 0 GPa transforms to a phase with symmetric hydrogen bond at 28 GPa. The first experimental investigation on hydrogen bond symmetrization in δ-AlOOH was done by Sano-Furukawa et al. [88] using a neutron diffraction experiment. Though they didn't observe symmetrization in their studied pressure regime up to 9.2 GPa, their linearly and quadratically extrapolated result predicted the hydrogen bond symmetrization pressure to be 16 and 24 GPa respectively. First principles calculations by Panero, and Stixrude [86] showed that the hydrogen bond in δ-AlOOH is symmetric at 0 GPa. However, this result was contradicted by Xue, and Kanzaki [89] where their Raman and Nuclear Magnetic Resonance (NMR) measurement on δ-AlOOH ruled out hydrogen bond symmetrization at ambient condition. An upper limit for hydrogen bond symmetrization was fixed by Li et al. [42] from their theoretical study. The change in hydrogen bonding, particularly the hydrogen bond symmetrization significantly affect the diagonal elastic constants where C_{11} and C_{22} exhibit anomalous behaviour across hydrogen bond symmetrization and hence the bulk modulus [43]. High-pressure X-ray [35] and neutron diffraction [88] studies reported a change in compressibility accompanied by hydrogen bond symmetrization in δ-AlOOH below 10 GPa. Similar changes in the compressibility of δ-AlOOH below 10 GPa was reported by Kuribayashi et al. [80] without any hydrogen bond symmetrization up to 10 GPa, which shows that the compressibility change is not driven by hydrogen bond symmetrization. They also observed disappearance of some Bragg reflections and attributed this to $P21nm \rightarrow Pnnm$ structural transition of δ-AlOOH between 6.1 and 8.2 GPa. However, synchrotron X-ray powder diffraction study of δ-AlOOH by Vanpeteghem et al. [84] didn't observe structural phase transition up to 22.5 GPa.

A recent sound velocity measurement on δ-AlOOH using Brillouin spectroscopy up to 134 GPa showed an increase in acoustic velocities of δ-AlOOH from 6 to 15 GPa [44], which has geological implications such as the cause of anomaly in shear velocity beneath the Korean peninsula. However, the study by Mashino et al. [44] highlights the discrepancies among experimental and theoretical results in determining hydrogen bond symmetrization pressure as well as the pressure induced structural transition reported by Kuribayashi et al. [80]. Hence, we investigate the structural evolution of δ-AlOOH at ambient and high-pressures using first principles calculation based on density functional theory to determine the hydrogen bond symmetrization pressure and its effect on mechanical and vibrational properties of δ-AlOOH. Our results confirm the underlying assumption of hydrogen bond symmetrization to be responsible for the velocity jump in δ-AlOOH observed in reported sound velocity measurement. Further, the anomaly can be correlated to the velocity profile beneath Java subduction zone.

3.2 Methodology

The high-pressure study on δ-AlOOH was carried out using first principles calculations based on density functional theory (DFT) [61] as implemented in the Quantum Espresso simulation package [90, 91]. The exchange-correlation functional was treated using local density approximation (LDA) as proposed by Perdew, and Wang [92]. The cut-off value of energy for plane wave basis set to expand the electronic wave function was determined to be 140 Ry after performing the convergence test. Brillouin zone sampling was done using the Monkhorst Pack grid of dimension 6×6×10. The choice of LDA over other approximations to exchange-correlation functional was made due to the non-implementation of the later in the PWSCF code for calculation of Raman intensity. The structural relaxation was performed employing Broyden-Fletcher-Goldfarb-Shanno (BFGS) [93] algorithm under the condition of maximum Hellmann-Feynman force acting on each atom to be less than 0.001 eV/Å. Vibrational properties were calculated using Density Functional Perturbation Theory (DFPT) [94] as implemented in the Quantum Espresso code. The dynamical matrices were calculated on **q**-points sampled using a 6×6×10 grid. Elastic constants were calculated using the Elastic code [95] where 9 sets of deformed crystal structures were generated to calculate the second order derivative of stress.

3.3 Results and discussion

3.3.1 Structural properties

At ambient condition, δ-AlOOH exhibits orthorhombic symmetry with $P21nm$ space group as determined from X-ray powder diffraction study by Suzuki et al. [83] and the asymmetric nature of O-H--O configuration was confirmed from NMR study [89]. We initially performed geometrical optimization of δ-AlOOH at 0 GPa to study the ground state structural parameters in comparison with the reported data. The position of hydrogen atoms to initiate the geometrical relaxation was provided such as to satisfy the O-H bond length criteria of 0.81 Å as measured by Komatsu et al. [85]. The optimized geometry of δ-AlOOH yield asymmetric O-H--O configuration with O-H bond length of 1.08 Å. The calculated structural parameters is presented in Table. 3.1 which shows a

Table 3.1: Calculated structural parameters, elastic modulus, elastic constants and sound velocities of δ-AlOOH at 0 GPa.

	This work	Other works	
		Theory	Expt.
a (Å)	4.63	4.63[86],4.79[43]	4.72[84],4.71[83],4.71[80],4.71[44],4.72[85]
b (Å)	4.12	4.11[86],4.28[43]	4.23[84], 4.22[83], 4.22[80], 4.22[44], 4.22[85]
c (Å)	2.79	2.81[86],2.88[43]	2.84[84], 2.83[83], 2.83[80], 2.83[44], 2.83[85]
O-H (Å)	1.09	1.06[41],1.21[86]	0.81[85]
O--H (Å)	1.36	1.21[86]	1.74[85]
O--O (Å)	2.45	–	2.55[80]
V ($Å^3$)	53.22	53.59[86],56.96[43],57.72[42]	56.54[84],56.37[83],56.37[80],56.37[44], 56.34[85]
B (GPa)	190.22	230[86], 153, 216[42]	252.3[84], 124[83]
G (GPa)	166.15	130[43]	–
Y (GPa)	386.05	–	–
C_{11} (GPa)	397.00	314[43],416[42]	–
C_{22} (GPa)	409.60	306[43],509[42]	–
C_{33} (GPa)	448.50	391[43],418[42]	–
C_{44} (GPa)	146.90	117[43],133[42]	–
C_{55} (GPa)	140.20	115[43],124[42]	–
C_{66} (GPa)	201.40	152[43],229[42]	–
C_{12} (GPa)	53.70	34[43],137[42]	–
C_{13} (GPa)	92.60	95[43],93[42]	–
C_{23} (GPa)	82.20	67[43],84[42]	–
V_p (km/s)	10.48	9.82[43]	9.54[44]
V_s (km/s)	6.66	6.19[43]	5.89[44]
V_Φ (km/s)	7.12	6.73[43]	–

reasonable agreement of structural parameters at 0 GPa calculated in this study with reported data. However, comparatively lower values of lattice parameter as compared to experimental results are expected due to the over binding nature of LDA.

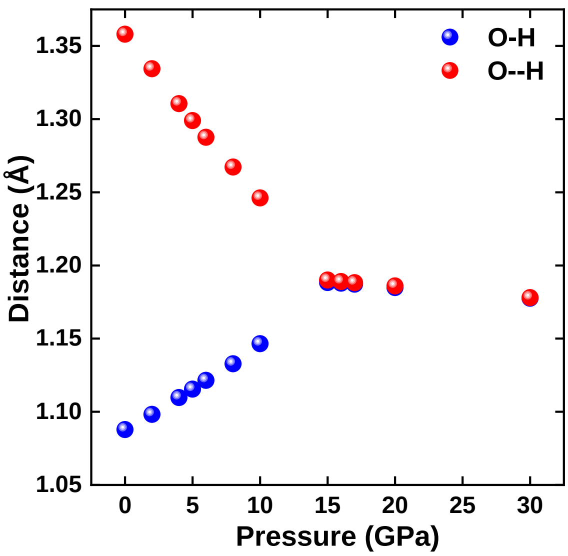

Figure 3.2: Pressure dependence of hydroxyl bond length (O-H) and and hydrogen bond (O–H).

The variation in O-H--O configuration of δ-AlOOH with pressure can be seen from the plot of pressure dependence of O-H and O--H in Fig. 3.2. The O-H and O--H bond length increases and decreases respectively with pressure and becomes identical at 15 GPa evidencing the formation of symmetric hydrogen bond. According to the perturbation molecular approach model, hydrogen bond length has a linear correlation with hydrogen bond strength which suggest that the hydrogen bond length increases in δ-AlOOH up to 15 GPa. However, above 15 GPa, the O-H--O configuration is nearly insensitive to pressure suggesting that the participating forces are under equilibrium and undergo identical contraction of both bond lengths owing to excessive compression. The observed evolution of O-H--O configuration and the participating forces is similar to that observed during VIII-X phase transition of ice [96]. Hence at 15 GPa, the covalent force (O-H bond), nonbonding dispersion force (O--H), and a third repulsive force arising from between the bonding electrons of O-H and nonbonding electron pair of O--H approaches equilibrium. The hydrogen symmetrization pressure obtained in this study is close to the experimentally predicted value of 15 GPa by Mashino et al. [44] and 16 GPa by Sano-Furukawa et al. [35], however, it is much lower than the theoretically predicted value of 30 GPa by Tsuchiya, and Tsuchiya [43] which might be attributed to the different approximation of exchange-correlation functional used. This also shows that the hydrogen bond symmetrization is sensitive to the functional used in DFT calculations.

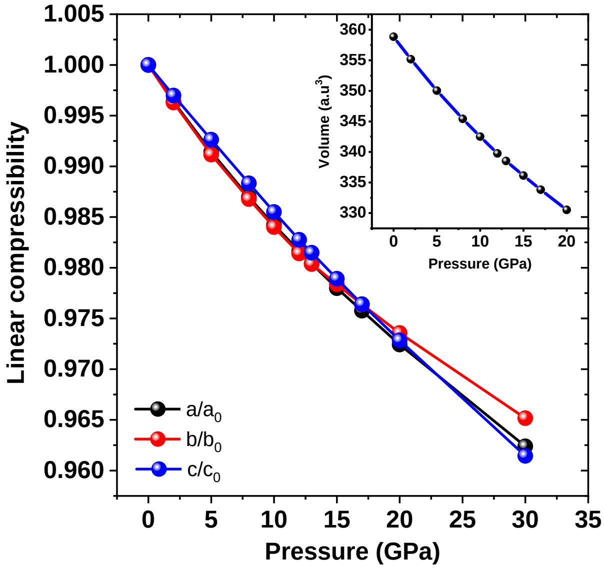

Figure 3.3: Evolution of linear compressibility with pressure for δ-AlOOH.

It is noteworthy that LDA, which is believed to underperform GGA, provides a promising result for the high-pressure behaviour of δ-AlOOH. One should note that LDA has been shown to describe the structural geometry of hydrogen bonding environment better than the estimation of its energy [97].

Further changes in pressure response of δ-AlOOH can be seen from the pressure dependence of compressibility as shown in Fig. 3.3. The compressibility along the c-axis indicates the compression of Al-O octahedral cages lying along the a direction and the compressibility of b and c lattice parameter is driven by the change in hydrogen bonds along the b-c plane. At low pressure, compression of the unit cell of δ-AlOOH along b and c direction undergoes relatively larger compression than that along a-direction. This shows that the b-c plane, hence the asymmetric hydrogen bonds along the b-c plane undergoes initial and large compression as compared to AlO_6 octahedra. This is consistent with the theoretical study of Tsuchiya et al. [41], however, contradicts the XRD study by Vanpeteghem et al. [84] where they showed that the unit cell of δ-AlOOH is more compressible along the c-axis accompanied by compression of O--O bond. With increase in pressure, the hydrogen bond strength increases and the compressibility of the b-c plane decreases than that along a direction. Fig. 3.3 shows that the crossover of all axial compressibility happens at 15 GPa, the hydrogen bond symmetrization pressure. There is no sudden change in volume across the hydrogen bond symmetrization pressure as

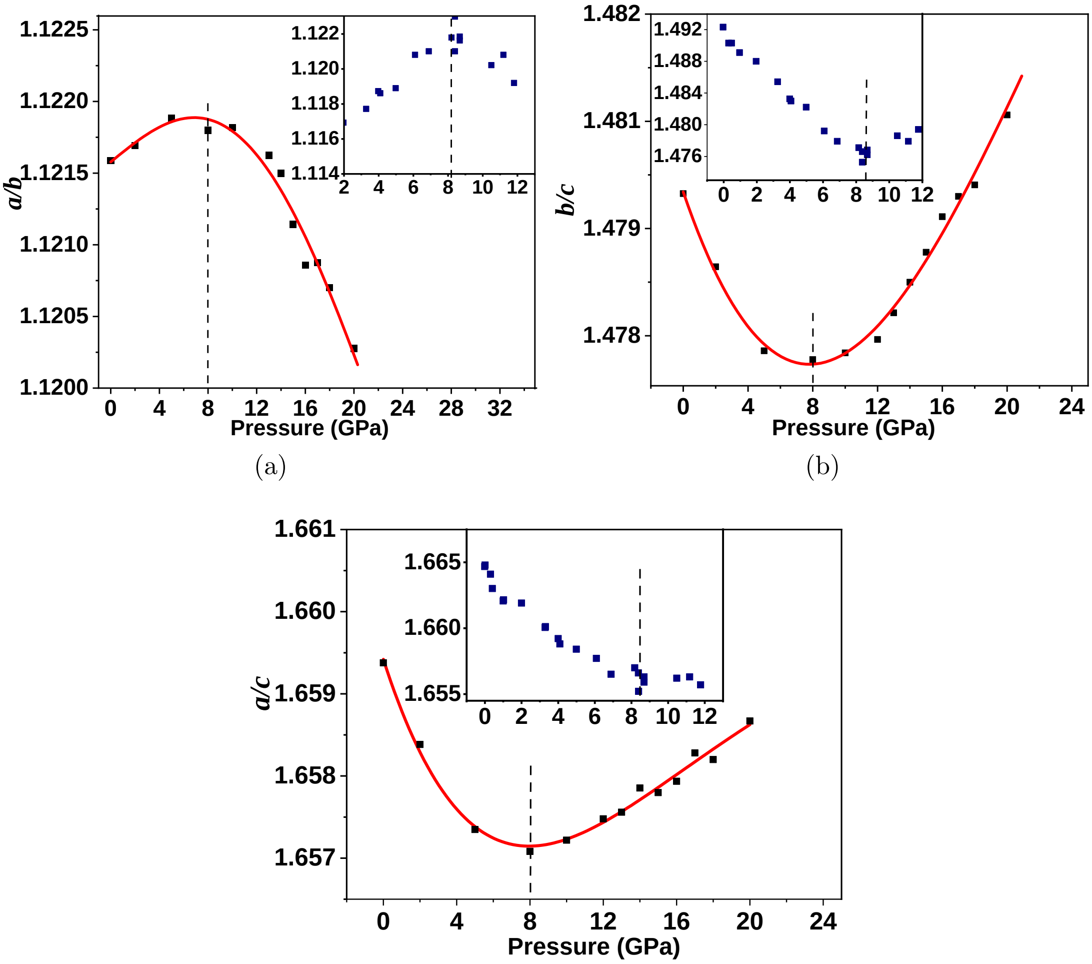

(c)

Figure 3.4: Change in relative compressibility of δ-AlOOH with pressure: (a) a/b, (b) b/c and (c) a/c. The inset shows the experimental data of δ-AlOOH from Kuribayashi et al. [80].

seen from the inset of Fig. 3.3. To investigate the pressure induced structural transition in δ-AlOOH from $P21nm$ to $Pnnm$ as reported in the single-crystal synchrotron XRD measurement by Kuribayashi et al. [80], we analysed the axial ratio (a/b,b/c and a/c) of the unit cell at each pressure values as shown in Fig. 3.4 and is compared with the reported experimental data [80]. All the axial ratios undergo slope change at 8 GPa. The b/c and a/c ratio decreases with pressure up to 8 GPa and increases above 8 GPa and as a consequence, an opposite trend is observed for a/b. It is noteworthy, that the observed turning point of axial ratio agrees well with that of Kuribayashi et al. [80]. The calculated O--O bond length in δ-AlOOH at 8 GPa is 2.4 Å which falls within the hydrogen tunnelling regime of 2.44–2.36 Å as classified by Benoit, and Marx [98]. Therefore, both the minima

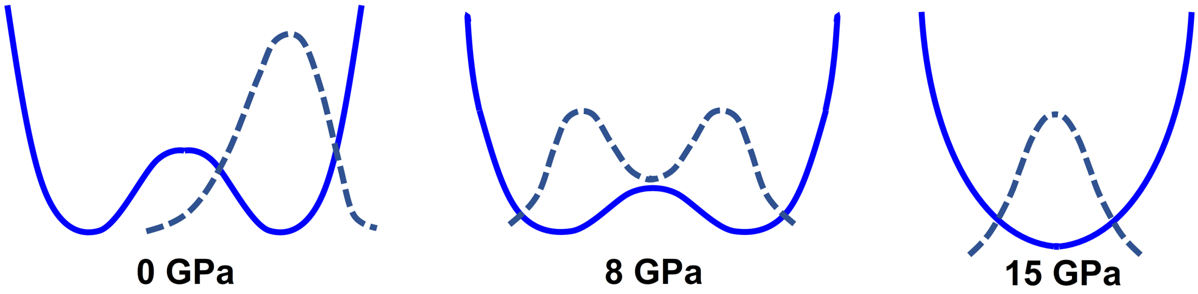

Figure 3.5: Illustration of probable evolution of potential well for O-H--O configuration with pressure in δ-AlOOH. (probability of locating a hydrogen atom is shown using dashed curves).

of potential energy surface lying between O--O pair has an equal probability of finding the hydrogen atom. This corresponds to a hydrogen disordered state consistent with the reported XRD study [80]. The structural transition pressure of 8 GPa is slightly lower than that determined by Sano-Furukawa et al. [35] (10 GPa). The space group of this disordered phase of δ-AlOOH has been determined to be *Pnnm* by Kuribayashi et al. [80]. The potential barrier decreases with further increase in pressure and transforms to an energy surface with a single minimum where the probability of locating hydrogen becomes maximum, as illustrated in Fig. 3.5, leading to hydrogen bond symmetrization.

3.3.2 Elastic properties

Recent Brillouin zone spectroscopic measurement attributed the observed anomalous behaviour of the acoustic velocity in δ-AlOOH to hydrogen bond symmetrization. To investigate the experimentally observed changes in sound velocities, we studied the pressure dependence of elastic constants and moduli, which strongly influences the sound velocity of a material. The orthorhombic unit cell of δ-AlOOH has 9 elastic constants and are presented in Table 3.1 which agrees well with the reported values. The pressure dependence of elastic constants of δ-AlOOH is shown in Fig. 3.6. Among nine elastic constants, C_{11}, C_{22}, C_{12}, C_{23} and C_{13} shows a sudden increase in their values across hydrogen bond symmetrization pressure indicating a significant effect of hydrogen bonding on elastic constants, whereas, the shear components C_{44}, C_{55} and C_{66} do not show any anomalous behaviour across the symmetrization pressure. The anomalous behaviour of

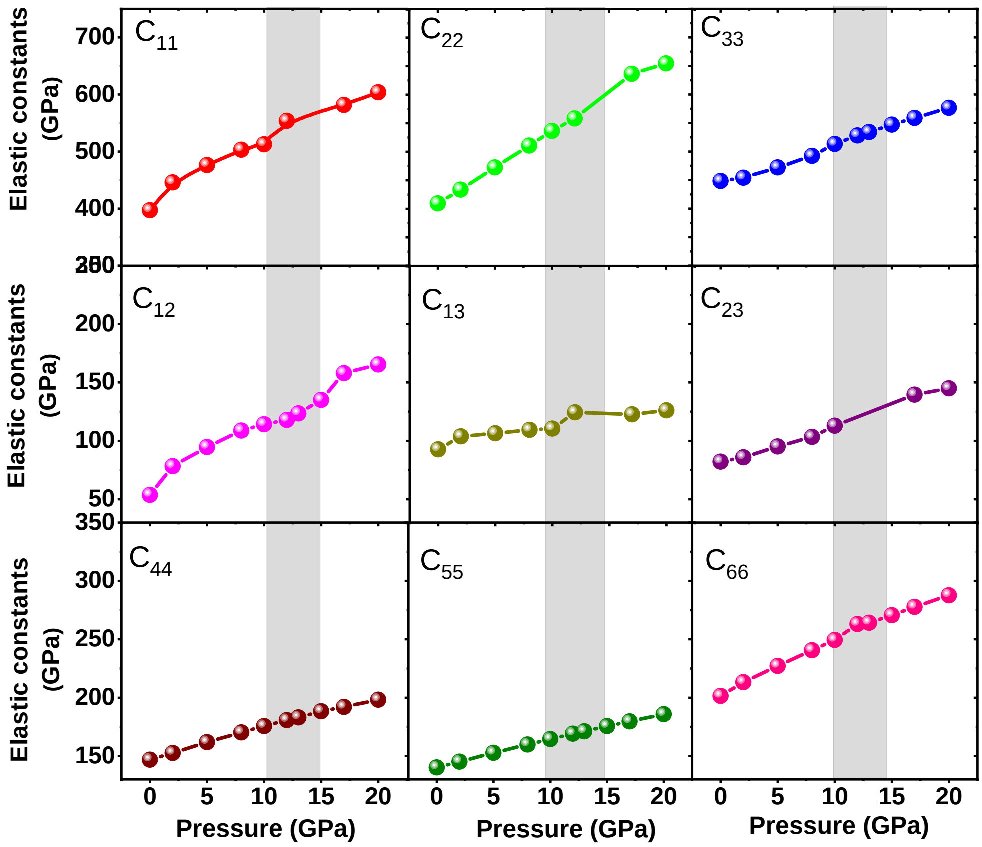

Figure 3.6: Variation of elastic constants of δ-AlOOH with pressure. The highlighted regions corresponds to the anomalous behaviour of elastic constants.

elastic constants leads to a steep increase in bulk (B) and Young's (Y) modulus as shown in Fig. 3.7(a). To estimate the effect of hydrogen bond symmetrization in bulk and Young's modulus quantitatively, the pressure derivative (Pr. Drv) of elastic moduli above and below the symmetrization pressure is presented in Table 3.2. Further, consistent with the behaviour of the shear component of elastic constant, the shear modulus (G) does not show anomalous behaviour in the studied pressure regime and the change in pressure derivative is relatively very small across the symmetrization pressure.

Table 3.2: Pressure derivative (Pr. Drv) of elastic moduli of δ-AlOOH.

Elastic modulii	Pr.Drv below 15 GPa	Pr.Drv above 15 GPa
Y	7.78	10.32
B	4.70	15.09
G	3.16	2.42

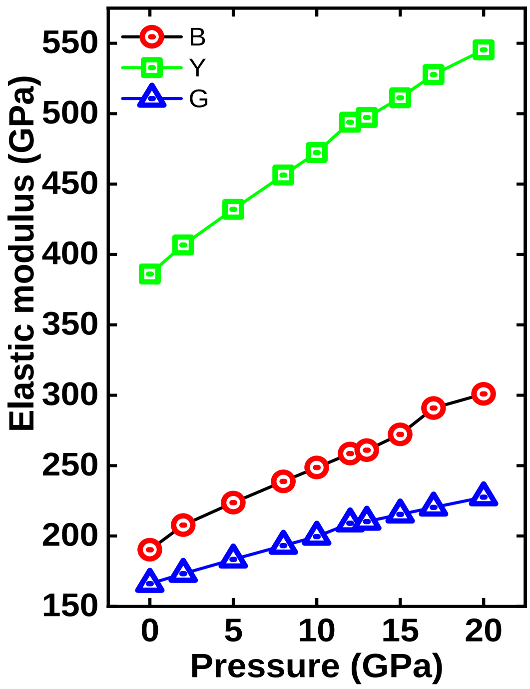

(a)

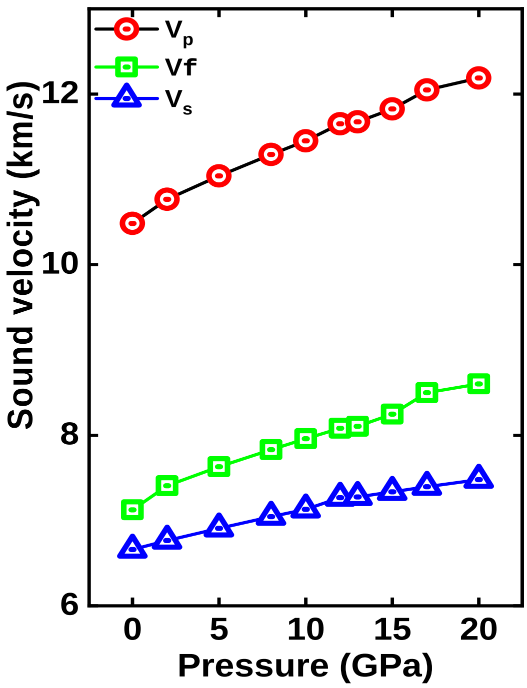

(b)

Figure 3.7: (a) Variation in elastic modulus, (b) bulk (V_Φ), shear (V_s) and longitudinal (V_p) sound velocities of δ-AlOOH with pressure.

The elastic modulli can be used to determine the longitudinal (V_p), bulk (V_Φ), and shear (V_s) wave velocities using the following set of equation:

$$V_p = \sqrt{\frac{B + \frac{4}{3}G}{\rho}} \quad V_\phi = \sqrt{\frac{B}{\rho}} \quad V_s = \sqrt{\frac{G}{\rho}} \tag{3.1}$$

where ρ is the density of δ-AlOOH. The variation in sound velocities under pressure is shown in Fig. 3.7 (b). The sound velocities show steep increase in symmetrization pressure regime which is an artifact of the changes observed in elastic constants. This validates the conclusion drawn from the sound velocity measurement in δ-AlOOH by Mashino et al. [44] and we confirm that the hydrogen bond symmetrization in δ-AlOOH is responsible for positive anomaly reported in sound velocity measurement.

3.3.3 Vibrational properties

The hydrogen bond symmetrization in δ-AlOOH were further studied using vibrational modes and Raman spectrum calculated using DFPT. The experimentally reported Raman spectrum of δ-AlOOH at ambient condition has four broad peaks in high frequency range corresponding to stretching vibrations of hydroxyl group [81, 89, 99]. However, Kudoh et al. [100] attributed two of the Raman peaks to different O--O bond lengths whereas Xue, and Kanzaki [89] attributed the multiple broad bands to Fermi resonance among fundamental O-H stretching mode and overtones. δ-AlOOH has 8 atoms per unit cell and therefore has 24 modes of vibration. The irreducible representation of the assymetric phase of δ-AlOOH is:

$$\Gamma = 7\mathrm{A}_1 + 4\mathrm{A}_2 + 3\mathrm{B}_1 + 7\mathrm{B}_2$$

and that of symmetric phase of δ-AlOOH is

$$\Gamma = 2\mathrm{A_g} + 2\mathrm{B_{1g}} + \mathrm{B_{2g}} + \mathrm{B_{3g}} + 3\mathrm{A_u} + 2\mathrm{B_{1u}} + 5\mathrm{B_{2u}} + 5\mathrm{B_{3u}}$$

where $\mathrm{B_{3g}}$, $\mathrm{B_{2g}}$, $\mathrm{B_{1g}}$ and $\mathrm{A_g}$ represents Raman active modes. The symbols A, B u, and g stands for degenerate mode, non-degenerate mode, Raman and Infrared activity respectively. The calculated Raman spectrum showed two intense peaks at 1870 and 2117 cm^{-1} which are within the O-H stretching region of 1000 to 3500 cm^{-1} [101]. Since the unit cell of δ-AlOOH consists of four O-H group, the two high-frequency modes can be assigned to the coupled stretching vibration of neighbouring O-H bonds related to identical O--O distance. A similar assignment of bands was done for the low pressure AlOOH polymorphs; boehmite and diaspore [102]. The evolution of vibrational modes with pressure is shown in Fig. 3.8.

Two pressure regimes can be identified for the high-pressure behaviour of O-H stretching frequency mode. The frequency of O-H stretching mode decreases initially with pressure and begins to increase above 15 GPa, the hydrogen symmetrization pressure. The transition of O-H frequency mode from the softening to the hardening of O-H stretching frequency distinguishes the asymmetric and symmetric phases of δ-AlOOH and can serve as spectroscopic evidence. Further, we calculated the intensity of Raman active modes and is presented in Fig. 3.9. The main changes observed in hydrogen bond symmetrization is the disappearance of the peaks corresponding to O-H stretching vibrations, suggesting that O-H stretching vibration of symmetric phase of δ-AlOOH are Raman inactive. measurements. Further, changes are also observed in low frequency region across the

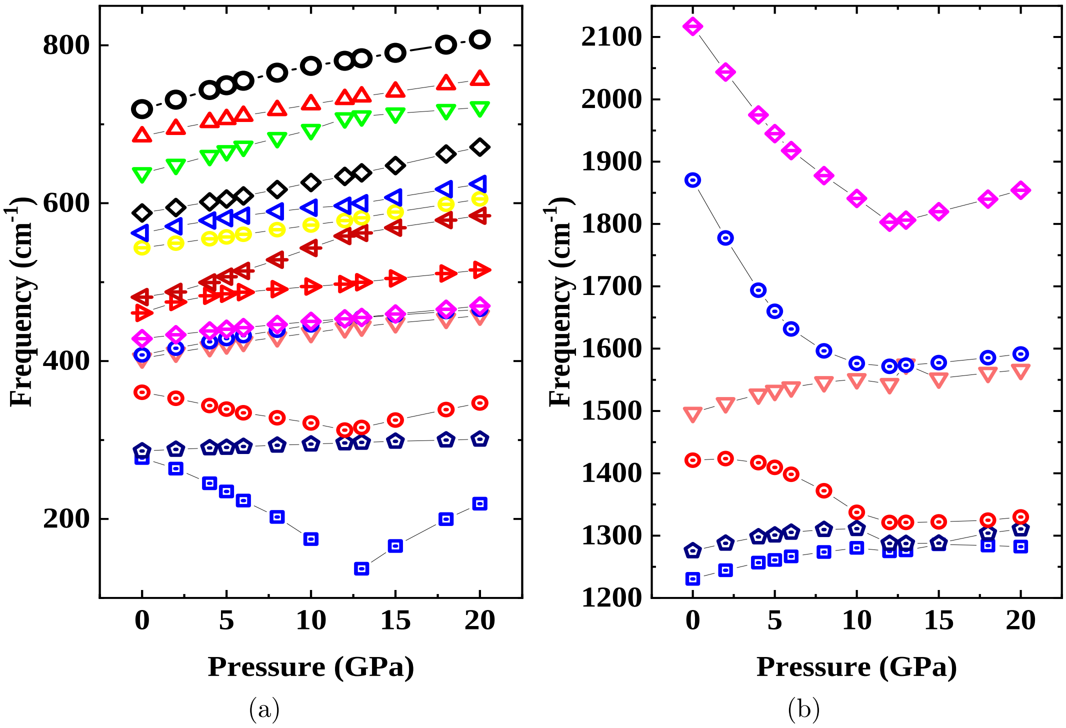

Figure 3.8: Evolution of zone center phonon modes of δ-AlOOH with pressure. For clarity of presentation, low and high frequency regime is presented in (a) and (b) respectively.

*P*21*nm* to *Pnnm* phase transition where the Raman band at 200-400 cm^{-1} disappears at 5-8 GPa, accompanied by the appearance of a new peak at 500 cm^{-1}. This characteristic Raman band of *Pnnm* phase can be assigned to A_g mode consistent with the Raman spectroscopic measurement by Mashino et al. [44]. Both the transitions, *P*21*nm* to *Pnnm* transition and asymmetric to symmetric transition of δ-AlOOH can be captured using Raman spectrum measurement. The phonon modes throughout the Brillouin zone were calculated and plotted in Fig. 3.10. The absence of any imaginary phonon modes confirms the lattice dynamical stability of symmetric phase of δ-AlOOH at 15 GPa.

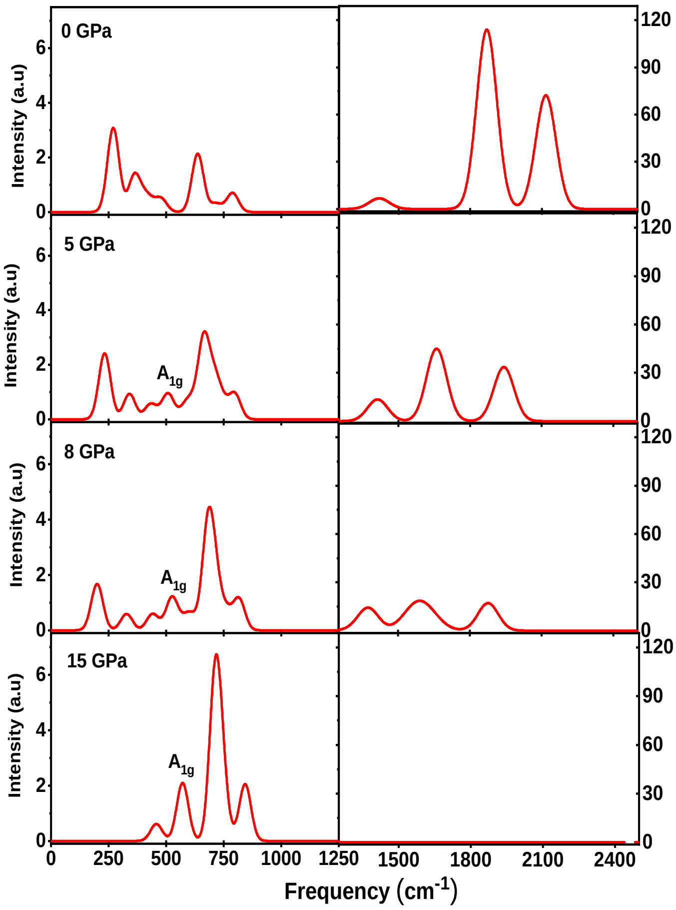

Figure 3.9: Pressure dependence of calculated Raman spectrum of δ-AlOOH. (For clarity, low and high frequency Raman modes are presented using different scales.)

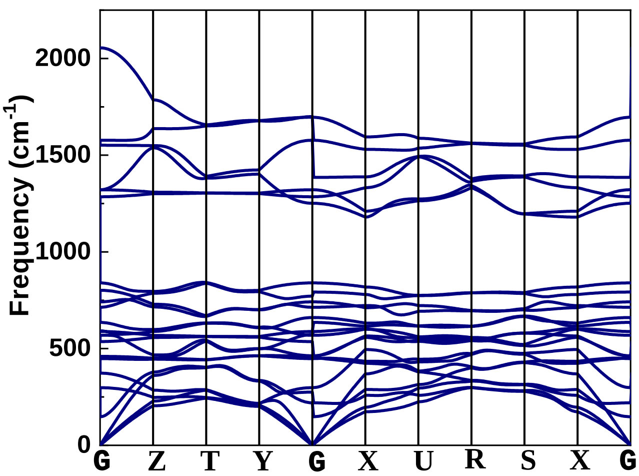

Figure 3.10: Calculated phonon dispersion curves at 15 GPa of δ-AlOOH.

3.4 Geophysical implications

The sound velocity measurement in δ-AlOOH by Mashino et al. [44] could explain the observed V_s anomaly reported beneath the Korean peninsula at a depth of 600 km and a negative shear velocity anomaly near the northern margin of the large low-shear-velocity province at a depth of 2800 km in the lowermost mantle beneath the Pacific. Thus, δ-AlOOH affects the propagation of seismic waves particularly at depths which favours the condition for hydrogen bond symmetrization in δ-AlOOH. Even though seismic discontinuities at several depths are reported, only the primary discontinuities at 400 and 600 km have been observed globally which results from phase transformations of olivine into wadsleyite and ringwoodite into perovskite (post spinel) respectively [102, 103]. From the results of our high-pressure study on δ-AlOOH, we attempt to interpret the anomaly in the velocity profile reported at a depth ranging from 100 to 600 km under the Deccan Volcanic Province (DVP) in Central and West India [104]. The reported model however featured the high velocity zone confined in 100-400 km as distinct from 400-600 km as the latter was characterised by the diffused low velocity. The 100-400 km region of high-velocity is thicker than the conventionally accepted lithosphere thickness of 200 km. The influence of δ-AlOOH in the seismic structure of DVP cannot be ruled out given the deposits of bauxite ore in India that are enriched with aluminium hydroxide [105] and the velocity and shear modulus of δ-AlOOH being relatively higher among other dominant minerals [44]. Further, a depth of about 400 km corresponds to the pressure of 14-15 GPa which is favourable for hydrogen bond symmetrization in δ-AlOOH thereby contributing to the anomalous high-velocity structure. Similarly, the velocity anomaly in δ-AlOOH could be correlated with the high-velocity anomaly in the Java subduction zone where the Mesozoic oceanic lithosphere undergoes subduction up to a depth of 1200 km having high velocity anomalies reported at a depth of 1000 km [106]. The tomographic visualization displaying the subduction of the Indo-Australian plate beneath the western Java Island has been conducted by Listyaningrum et al. [106]. Their obtained tomographic profile shows an increase in the velocity (V_p) throughout the subducting slab as seen from Fig. 3.11. The presence of δ-AlOOH carried among the sediments by subducting slabs could have implications to the observed increase in velocity in the Java subduction zone and a similar conclusion holds for various subduction zones where the subducting slab carries sediments to the depth within the stability field of δ-AlOOH.

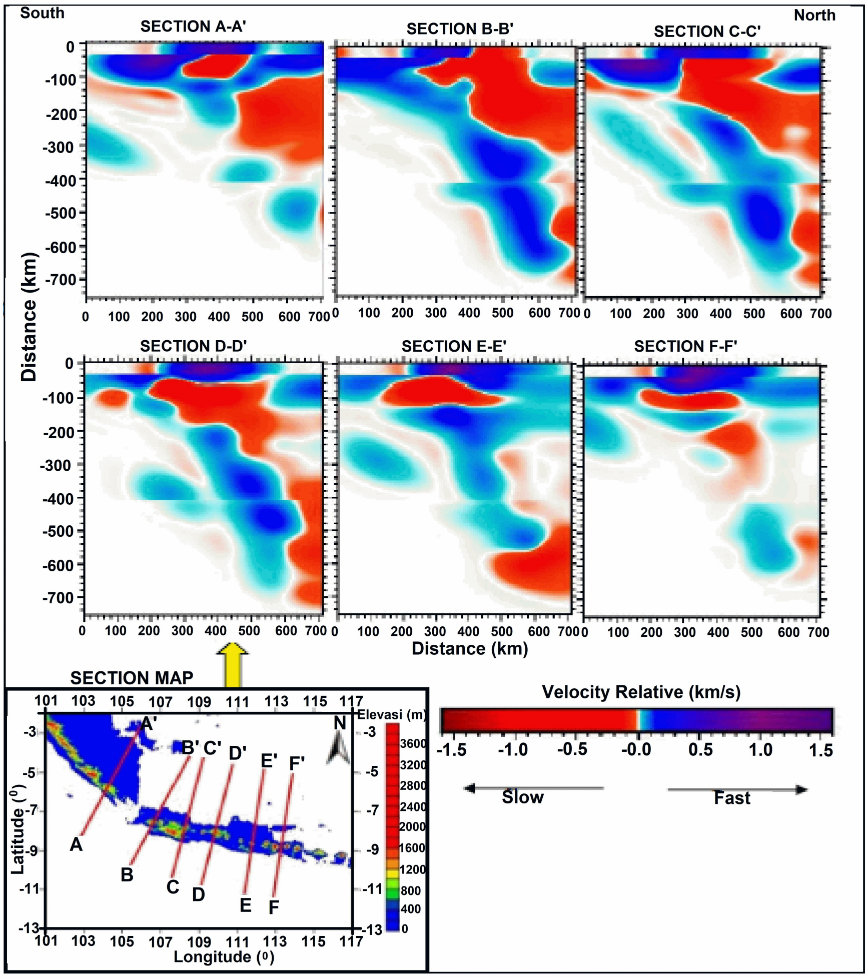

Figure 3.11: The tomographic data presenting the subduction of Indo-Australian plate beneath the Western Java Island. Red colour indicates a reduction of velocity by –5%. The blue colour indicates an increase in velocity by +5% (Ref. Listyaningrum et al. [106]).

3.5 Conclusions

We determined the pressure at which δ-AlOOH transforms from the structure characterised by an asymmetric hydrogen bond to phase with symmetric hydrogen bond through an intermediate stage of $P21nm$ to $Pnnm$ structural phase transition. Further, the influence of hydrogen bond symmetrization on the elastic properties and vibrational properties were studied. First principles calculations based on density functional theory employing local density approximation to exchange-correlation functional shows the hydrogen bond symmetrization in δ-AlOOH occurs at 15 GPa. Further, the study provides the first theoretical support to the experimentally observed velocity anomaly in δ-AlOOH, consistent with lower hydrogen-bond symmetrization pressure reported experimentally as compared to previously suggested symmetrization pressure of 30 GPa from the DFT study [41]. At low pressure, O-H bond length increases and O--H hydrogen bond length decreases up to 15 GPa, beyond which, both bond length decreases at a constant rate. The evolution of O-H--O configuration in δ-AlOOH is similar to that observed during ice VIII-X phase transition [96], hence at 15 GPa, the covalent force (O-H bond), nonbonding dispersion force (O--H), and a third repulsive force arising from between the bonding electrons of O-H and nonbonding electron pair of O--H approaches equilibrium. Compressibility study shows that hydrogen bond lying parallel to *b*-*c* plane undergoes larger compression as compared to the AlO_6 octahedra lying along the *a* direction. At 15 GPa, the compressibility of hydrogen bond, and hence along *b*-*c* plane decreases due to strengthening of hydrogen bond and hence as a result, *c*-axis becomes more compressible above hydrogen bond symmetrization pressure. Further, the pressure dependence of axial ratio confirms the $P21nm$-$Pnnm$ phase transition at 8 GPa consistent with the XRD measurement reported by Kuribayashi et al. [80]. Thes hydrogen bond symmetrization significantly affects the elastic constants and hence the sound velocity in δ-AlOOH. The sound velocity shows anomalous increase across the hydrogen bond symmetrization pressure. Raman spectroscopic investigation shows that both asymmetric to symmetric phase change and the $P21nm$ to $Pnnm$ phase transition in δ-AlOOH can be characterised by the disappearance of Raman peak corresponding to O-H stretching vibration and appearance of Raman mode (A_g) at 500 cm^{-1} respectively. The velocity anomaly across symmetrization pressure in δ-AlOOH has geological implications where it can be related to the seismic anomalies observed beneath the Java subduction zone and Deccan Volcanic Provinces of India.